

Impact of Clock Skewness on Synchronized Sensor Clusters Operating with IEEE 802.15.4 MAC

Kenji Leibnitz, Naoki Wakamiya, and Masayuki Murata
Graduate School of Information Science and Technology, Osaka University
1-5 Yamadaoka, Suita, Osaka 565-0871, Japan

Abstract

In this paper we propose an analytical model for IEEE 802.15.4 in a clustered sensor network environment. We investigate the timing delay, when all nodes transmit synchronously and derive the distribution of the transmission time for the cluster members to the cluster head. Further, we study the effects of clock skewness from each sensor node on the total delay and show how time margins can be easily found to avoid collisions from different rounds. Finally, we discuss the possibility of scheduling logical subclusters in order to improve the performance regarding transmission time and success rate.

1 Introduction

With the recent developments in Micro Electro Mechanical System (MEMS) technology, large-scale networks of integrated wireless sensor nodes have become available [1]. By deploying networks of sensors, information about behavior, conditions, and positions of entities in an environment are gathered and forwarded to a sink for further processing. The nodes are equipped with a sensing device, radio transmitter, and are usually battery operated. Since they are designed to operate autonomously, they must be able to set up a communication network in an ad-hoc manner and be able to adapt to changes in the network topology, when individual nodes may fail due to exhausted energy resources. Conservation of energy is, thus, a key issue in the deployment of sensor networks. Most energy consumption is caused by the communication over the radio link [2].

Recently, several publications have shown the benefits of using clustering methods in order to save energy and prolong the lifetime of the network [3, 4]. In clustered sensor networks, the sensor nodes do not transmit their collected data to the sink, but to designated cluster heads which aggregate the data packets and send them directly or via multi-hop communication to the sink. Thus, choosing the appropriate sizes and number of clusters is essential for the performance of the network lifetime.

In order to enforce standardization among sensor devices, the Zigbee Alliance [5] was formed in 2002 as an association of companies to create a low-cost and low-power transmission standard for *wireless personal area networks* (WPAN). The Zigbee specifica-

tion defines the communication on the network layer and above, while the IEEE 802.15.4 standard [6] is adopted for the physical and *medium access control* (MAC) layers. On MAC layer, access to the channel is controlled with a *carrier sense multiple access with collision avoidance* (CSMA/CA) algorithm that is especially designed for WPAN. It supports different network topologies, such as star-shaped and peer-to-peer. Recently, there has been a growing number of publications dealing with the performance of IEEE 802.15.4 [7, 8, 9]. However, most analytical approaches of CSMA/CA consider the system to operate under steady state conditions. Our focus in this paper is on an application in which the transmission instants of each node are synchronized, i.e., all nodes simultaneously initiate their transmission attempt. This specific type of scenario is highly non-stationary and very harmful for CSMA/CA as shown for IEEE 802.11 WLAN [10].

In this paper we present an analytical model of the transmission delay for a cluster of sensor nodes. The model is based on a discrete-time, discrete-state Markov chain model and derive the distribution of the complete transmission time for a cluster of sensor nodes to the cluster head in Section 2. Furthermore, we study the effects of skewness of the clock timings of each sensor on the total delay in 3. Numerical results are given in Section 4 and the paper is concluded by an outlook on future work in Section 5.

2 Analysis of CSMA/CA

In this section, we briefly review the analytical model given in [11]. Basically, the analysis consists of two

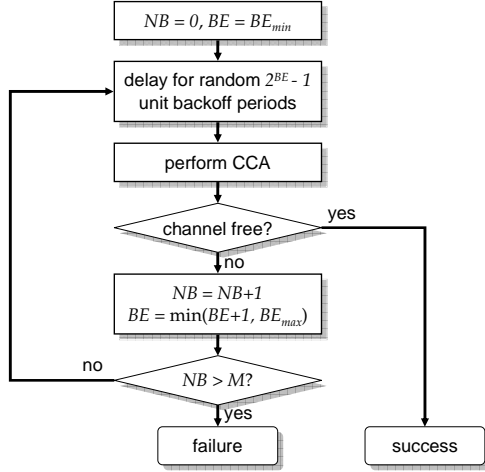


Figure 1: Flow chart of the CSMA/CA mechanism

parts: (i) determination of the attempt probabilities of each node, and (ii) computation of the time delay for transmitting and receiving. We focus on an application in which all nodes transmit synchronized every T_{sync} time periods.

We assume the sensor network to operate with the beacon-less mode according to the algorithm given in Fig. 1. The time axis is discretized into *backoff units*, each with a duration of 20 symbol periods. We consider the network to operate in the 2.4 GHz frequency band with a symbol rate of 62.5 ksymbols/s, hence, a backoff unit has a length of 80 bits. The variable BE denotes the *backoff exponent* that is increased from BE_{min} until BE_{max} . The variable NB indicates the *number of backoffs* and is initialized with $NB = 0$ at the beginning of each round. Default values in [6] are $BE_{min} = 3$, $BE_{max} = 5$ and the *maximum number of backoffs* is $M = 4$. If the transmission attempt has not been successful until the M -th backoff, it will be aborted. Note that the 0-th backoff is always performed. The *clear channel assessment* (CCA) is a physical layer primitive to check if the channel is busy or not. We incorporate the time required by CCA in our model by assuming that the transmission can start earliest at the next time slot after the attempt.

2.1 Attempt Probabilities

Let us consider a cluster with N nodes, each having a data packet of size L to transmit. At time $t = kT_{sync}$, $k \in \mathbb{N}$, all nodes attempt to transmit data packets to their cluster heads. Each backoff B_i for $i = 1, \dots, M$ is a uniform random variable less than W_i .

$$W_i = 2^{\min(BE_{min} + i, BE_{max})}$$

The backoff exponent size increases from BE_{min} to BE_{max} and the maximum number of backoffs is

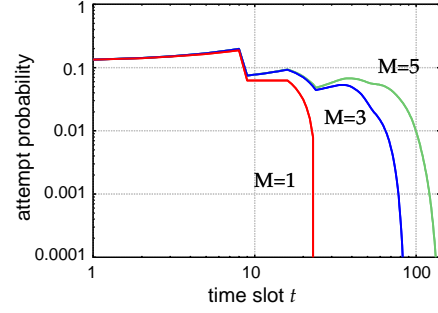


Figure 2: Attempt probability

denoted as M . Hence, we have each delay occurring with probability $d_i(t)$ for $i = 0, \dots, M$.

$$b_i(t) = P[B_i = t] = \frac{1}{W_i}$$

$$d_i(t) = P[B_0 + \dots + B_i] = b_0(t) \otimes \dots \otimes b_i(t)$$

The *attempt probability* $a(t)$ of each node is then simply the sum over all possible cases occurring at time $t \leq t_M$, with $t_k = \sum_{j=0}^k W_j$.

$$a(t) = \sum_{i=0}^M d_i(t) \quad (1)$$

The attempt probability for $N = 10$, $L = 2$ and different values of M is shown in Fig. 2. The curves all show the distinct sawtooth shape reported in [10]. However, due to the limited number of M , all curves decrease to zero for $t \rightarrow t_M$. Obviously, the attempt probability increases for large M .

2.2 Total Transmission Delay

We model the total transmission delay, i.e., the time from the synchronization instant until the final station has finished its transmission attempt, by using a discrete-time, discrete-state Markov chain state space as shown in Fig. 3.

The states are denoted by the number of unprocessed nodes and the time slots spent during transmitting. All transition probabilities are derived from the attempt probability $a(t)$ and are given as:

- the *success probability* $s_i(t)$ that one of the remaining i nodes is successful in its transmission attempt,

$$s_i(t) = i s(t) (1 - a(t))^{i-1}$$

- the *waiting probability* $w_i(t)$ that none of the nodes attempts a transmission,

$$w_i(t) = (1 - a(t))^i$$

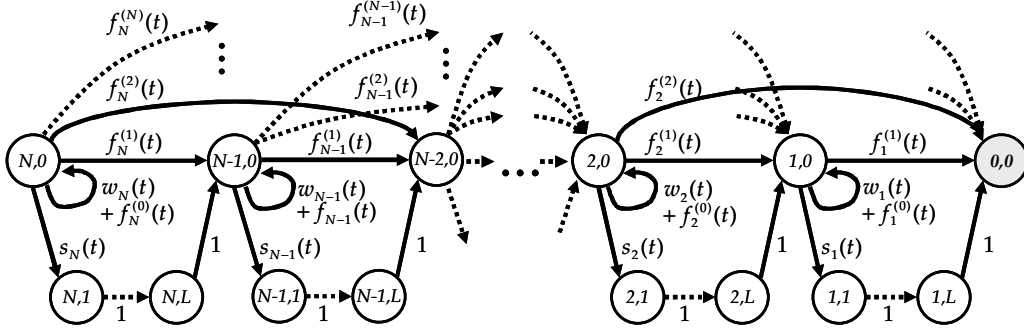


Figure 3: Markov chain state space

- the *collision probability* $c_i(t)$ as the complementary probability,

$$c_i(t) = 1 - (s_i(t) + w_i(t))$$

- and the *failure probability* $f_i^{(k)}$ that k nodes abort simultaneously,

$$f_i^{(k)} = c_i(t) \binom{k}{i} \eta^i (1 - \eta)^{k-i}$$

where $\eta = \min \left\{ 1, \frac{L(N-1)}{E[W]} \right\}$ is an approximation for the abort probability of each node.

As the attempt probabilities are time-dependent, we perform an iterative non-stationary analysis. Starting with initial vector

$$\mathbf{x}(0) = [0, \dots, 0, 1]$$

we multiply the state vector

$$\mathbf{x}(t) = [x_{i,j}(t)] \quad i = 0, \dots, N \quad j = 1, \dots, L$$

with the time-dependent transition matrix $\mathbf{P}(t)$ until $t = t_M$.

$$\mathbf{x}(t+1) = \mathbf{x}(t) \mathbf{P}(t)$$

The resulting component values $x_{0,0}(t)$ of vector $\mathbf{x}(t)$ constitute the cumulative probabilities of the total transmission delay T_{delay} . Examples of the distribution are illustrated in Fig. 4. The pale colored lines

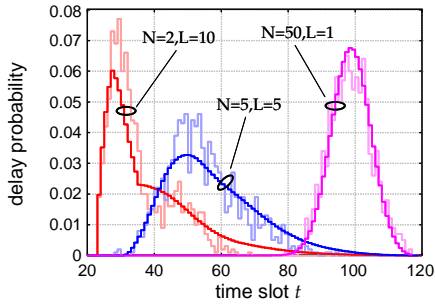


Figure 4: Total delay distribution

show the distributions obtained from simulations. It can be seen that the boldly colored analytical results match well with the simulation values.

2.3 Probability of Success

We are interested in the probability of a transmission attempt being successful until $t = t_M$. Since our Markov model does not distinguish between successful and aborted attempts, we obtain the number of successful nodes S_N after the round from a modified state space of Fig. 3 where we only distinguish between transitions for successful and unsuccessful attempts. From the state probabilities $x_{i,j}(t_{max})$ we then derive the *success probability* $\varphi_N = \frac{S_N}{N}$. The average number of successful transmissions and success probability are given in Eqn. (2).

$$S_N = \sum_{i=0}^N \left((N-i) \sum_{j=0}^L x_{i,j}(t_{max}) \right) \quad (2)$$

The number of successful nodes is shown in Fig. 5 over the total number of nodes. We varied the number maximum backoff M in this experiment. It can be clearly seen that increasing the number of nodes leads to a point after which the performance decreases due to collisions. Further, the figure gives a justification for using clustering methods and shows that the best

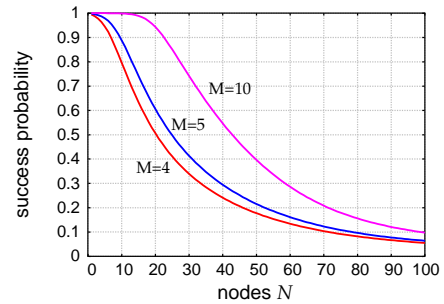


Figure 5: Success probability φ_N

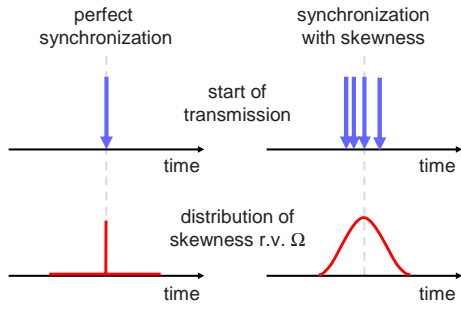


Figure 6: Model of clock skewness

operating range for IEEE 802.15.4 is up to approximately 20 nodes. A large M increases the capacity of the cluster, however, the value $M = 10$ used here is only a hypothetical value, as the standard in [6] specifies a limitation of $M \leq 5$. The success probability can be influenced similarly by increasing BE_{min} and BE_{max} .

3 Model of Clock Skewness

So far we modeled the total CSMA/CA delay while considering perfect synchronization among all nodes. However, in reality this can never be fully achieved, since there will always be a skewness of the internal clocks. In this section, we extend the model to include the effects of skewness in the clock timings on the performance of the transmission delay. The basic mechanism that we follow is sketched in Fig. 6.

Let us consider the timing offset as a random variable Ω . We model Ω as discretized normal distributed r.v. with mean $E[\Omega] = 0$ and variance $\omega = Var[\Omega]$. Examples of the cumulative distribution function are shown for different variance values in Fig. 7.

If we add the offset to the initial backoff window B_0 we obtain new attempt probabilities as shown in Fig. 8. Note that the plot denoted with $\omega = 0$ corresponds to the case with perfect synchronization as described in Section 2. It can be seen that when increasing ω , the sawtooth shape gets smoothed out and

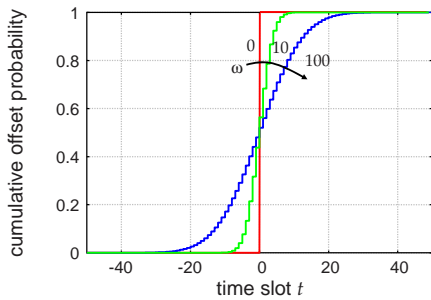


Figure 7: Cumulative skewness probabilities

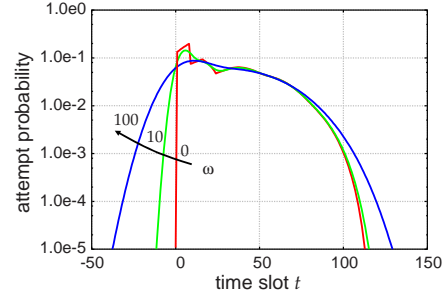


Figure 8: Attempt probabilities with skewness

the shape is dominated by the normal distribution.

We use these new attempt probabilities with the Markov model in the same way as described in Section 2.2 to obtain the transmission delays T_{delay} . The cumulative distributions of the corresponding curves in Fig. 4 are depicted for different values of ω in Fig. 9.

It can be seen that increasing the variance has a beneficial effect on the total delay as it spreads the timing of the first attempt over a longer period, so that collisions especially in the 0-th backoff phase do not occur so frequently with higher ω . However, this effect is reversed for large N . In the next section we investigate the effects of variation of the skewness in greater detail.

4 Numerical Results

The first question we wish to investigate in this section can be formulated as: *Is less time required if we schedule the transmissions for all nodes or sequentially for groups of nodes?* This would mean that we can split a physical cluster into several logical subclusters and perform their transmissions at different offsets. Another important question that we wish to examine is how does the clock skewness influence the transmission time. *Is it even more beneficial to have a high timing skewness in order to avoid collisions especially during the first backoff?*

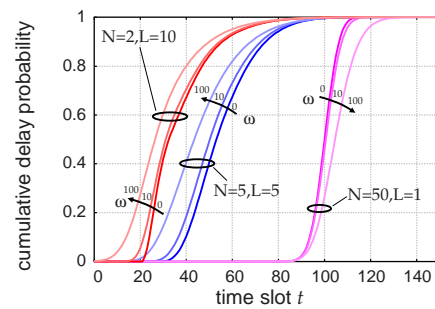


Figure 9: Delay CDF with skewness

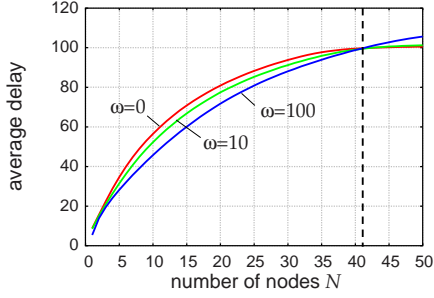


Figure 10: Average delay for $L = 1$

4.1 Benefiting from Time Skewness

When we consider clock skewness, the nodes may transmit prior to the actual synchronization instants. Therefore, we must take care that the synchronization time interval is large enough that no overlapping occurs as this would introduce additional unnecessary collisions. This is avoided by introducing a time margin T_{margin} and in this section we investigate the best choice for T_{margin} when the variance of the skewness ω is known. The idea is that if we intentionally add a certain clock skewness, we can in fact improve the system performance.

Let us consider the average delay for $L = 1$ in Fig. 10. We can see that increasing the variance of the clock skewness does indeed reduce the average transmission time up to a certain number of nodes (in this case about 41). Beyond this number of nodes, the effect is reversed in that the increased skewness yields a larger average time.

We varied ω in Fig. 11 and see that for $N = 10$ increasing the skewness variance has the same effect for different L except that the curves are shifted.

4.2 Optimal Time Margin

Let us now consider the appropriate choice of the time margin T_{margin} . Recall from Fig. 8 that for large ω there is a high probability of attempting prior to the actual synchronization time instant. This is caused by the normal distributed skewness variable Ω . For

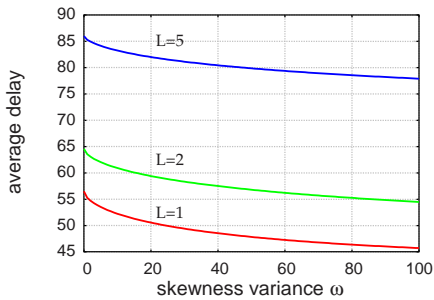


Figure 11: Influence of the skewness variance ω

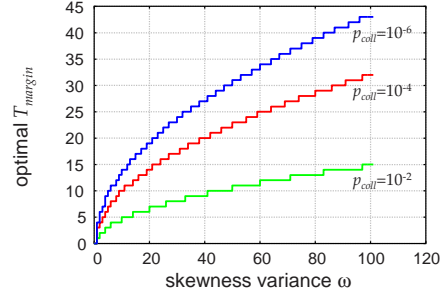


Figure 12: Optimal time margin for different p_{coll}

a given Ω with variance ω we consider T_{margin} to be sufficiently large if the probability of collisions from different rounds is below p_{coll} . In Fig. 12 the optimal values for T_{margin} are shown for $p_{coll} = 10^{-2}$, 10^{-4} , and 10^{-6} .

The optimal time margin certainly increases with stricter collision probability p_{coll} . Furthermore, if the skewness has a higher variance, the time margin must also increase. From curves like in Fig. 12, we are able to extract the optimal T_{margin} when p_{coll} and ω are given. Note that these values are minimum values. Choosing a larger margin than those obtained in this section does not harm the performance except for adding extra delay when we consider the scheduling of subclusters as shown in the following section.

4.3 Scheduling of Sensor Subclusters

Let us now investigate the question if it is better to split the cluster into two logical subclusters that are scheduled sequentially, see Fig. 13. In this example the transmission time is sketched in the top part for T_{sync} when all N nodes in the cluster start their transmission at the same instant. Our goal is to determine the time gain, if we split the cluster into two subclusters with $N/2$ nodes. A positive gain would justify the scheduling of subgroups in the cluster.

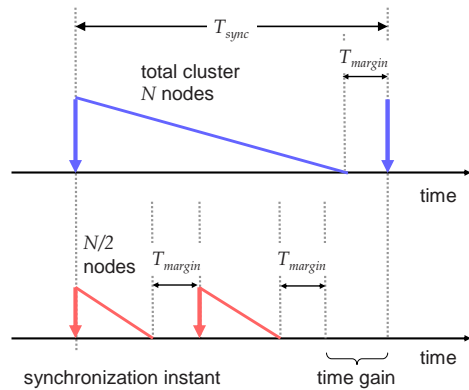


Figure 13: Timings with scheduling subclusters

Examining the shape of the curves with the average delay easily gives us an answer to the question if we can improve the average delay by forming subclusters. As the shape of the curve is concave, for any value N , smaller values than N always have a delay that is greater than half of the delay of N . For very large N , however, the slope levels out. We do not consider these values, as they show a high rate of failures due to collisions, see Fig. 5. In fact the only benefit we can gain from forming subclusters is that a higher percentage of nodes can be received successfully. From the viewpoint of the transmission delay we can not obtain any significant benefit.

5 Conclusion

In this paper we presented a model for clock skewness in a synchronized IEEE 802.15.4 sensor node cluster. The model uses a discrete-time, discrete-space Markov chain to evaluate the transmission delay of the whole cluster. The computation of the delay consisted of two parts: first the attempt probability was assumed independently for each user, and secondly, the total CSMA/CA access process was modeled.

Furthermore, we modified the model of perfect synchronization by adding a skewness offset modeled with a normal distributed random variable. It could be seen that introducing a certain skewness improves the average delay time for the transmission of a round. On the other hand, we found that when we exceed a limit on the number of nodes, this effect is reversed and turns into a disadvantage leading to increased delays. We also showed how time margins can be easily found that ensure that collisions from different rounds occur only at a very low probability.

Finally, we examined the questions, whether the splitting of a cluster into logical subclusters shows any benefit on the transmission time. We have discussed that while the average delay is not reduced, the partition into logical subclusters may lead to a lower failure rate. In this paper we only examined the possibility of splitting the cluster into two logical subclusters. In the future we wish to investigate a general fraction. This and the influence of collisions from other clusters are subject to further study.

Acknowledgment

This research was supported by “The 21st Century COE Program: *New Information Technologies for Building a Networked Symbiosis Environment*” and a Grant-in-Aid for Scientific Research (A)(2) 16200003 of the Ministry of Education, Culture, Sports, Science and Technology in Japan.

References

- [1] I. Akyildiz, W. Su, Y. Sankarasubramaniam, and E. Cayirci, “A survey on sensor networks,” *IEEE Communications Magazine*, vol. 40, no. 4, 2002.
- [2] W. Ye, J. Heidemann, and D. Estrin, “An energy-efficient MAC protocol for wireless sensor networks,” in *Proc. of IEEE INFOCOM*, (New York, NY), June 2002.
- [3] W. Heinzelman, A. Chandrakasan, and H. Balakrishnan, “An application-specific protocol architecture for wireless microsensor networks,” *IEEE Transactions on Wireless Communications*, vol. 1, no. 4, 2002.
- [4] J. Kamimura, N. Wakamiya, and M. Murata, “Energy-efficient clustering method for data gathering in sensor networks,” in *First Workshop on Broadband Advanced Sensor Networks (BaseNets)*, (San Jose, CA), Oct. 2004.
- [5] Zigbee Alliance. <http://www.zigbee.org/>.
- [6] IEEE 802.15.4, “Wireless Medium Access Control and Physical Layer Specifications for Low-Rate Wireless Personal Area Networks,” 2003.
- [7] M. Achir and L. Ouvry, “Power consumption prediction in wireless sensor networks,” in *ITC Specialist Seminar on Performance Evaluation of Wireless and Mobile Systems*, (Antwerp, Belgium), Aug. 2004.
- [8] G. Lu, B. Krishnamachari, and C. Raghavendra, “Performance evaluation of the IEEE 802.15.4 MAC for low-rate low-power wireless networks,” in *Workshop on Energy-Efficient Wireless Communications and Networks (EWCN '04)*, (Phoenix, AZ), 2004.
- [9] J. Misić, S. Shafi, and V. Misić, “Performance of 802.15.4 beacon enabled PAN in saturation mode,” in *Symposium on Performance Evaluation of Computer and Telecommunication Systems (SPECTS)*, (San Diego, CA), July 2004.
- [10] C. Foh and M. Zukerman, “Performance evaluation of IEEE 802.11,” in *IEEE Vehicular Technology Conference (VTC) Fall*, (Atlantic City, NJ), Oct. 2001.
- [11] K. Leibnitz, N. Wakamiya, and M. Murata, “Modeling of IEEE 802.15.4 in a cluster of synchronized sensor nodes,” in *submitted to 19th International Teletraffic Congress (ITC-19)*, (Beijing, China), 2005.